

Level-Set Segmentation of Arterial and Venous Vessels based on ToF-SWI data

A. Deistung¹, M. Strzelecki², A. Materka², and J. R. Reichenbach¹

¹Medical Physics Group, Department of Diagnostic and Interventional Radiology, Jena University Hospital, Jena, Germany, ²Institute of Electronics, Technical University of Lodz, Lodz, Poland

INTRODUCTION

Non-invasive quantitative assessment of the cerebral vasculature is of high diagnostic and therapeutic interest. Prerequisite for quantitative description of blood vessels is voxel-wise classification of angiographic data sets into vessel and non-vessel structures. Among the vast of algorithms suitable for vessel segmentation [1, 2] the level-set technique has been established as a flexible segmentation approach that handles morphological variations [3]. The level-set method enables iterative evolution of an initial curve towards boundaries of target objects driven by combining internal (geometry of evolving curve) and external forces (produced by the data). In this contribution, we use a hybrid level-set approach [4] that relies on both boundary and region information to create a 3D representation of the arterial and venous vasculature.

MATERIAL AND METHODS

Data Acquisition: High-resolution angiographic volunteer data of the whole brain were acquired with the dual-echo ToF-SWI sequence [5] ($TE_1/TE_2/TR/FA=3.43\text{ ms}/25\text{ ms}/42\text{ ms}/20^\circ$, $BW_1 = 296\text{ Hz/px}$, $BW_2 = 80\text{ Hz/px}$, voxel size = $0.45 \times 0.45 \times 1.2\text{ mm}^3$) on a 3T MRI system (TIM Trio, Siemens Medical Solutions, Erlangen, Germany) using a 12 channel head-matrix coil. The first echo of the ToF-SWI sequence collects time-of-flight (ToF) MR data, whereas susceptibility weighted imaging (SWI) data is acquired with the second echo. Signal saturation due to slowly flowing arterial blood in the ToF-part was reduced by using the multiple overlapping of thin slabs acquisition (MOTSA) technique with three slabs and a slab overlapping factor of -25 %. Venous saturation pulses were applied to reduce venous contamination in the ToF echo.

Data Pre-Processing: The multiple slabs were concatenated in image space as described in reference [5]. Phase data from the second echo was corrected by homodyne filtering [6] and regions with incompletely removed phase wraps were eliminated based on local field gradients [7]. In order to enhance venous vessel delineation susceptibility weighted images were calculated from the second echo by fourfold multiplication of the unwrapped weighted phase (phase mask) with the corresponding magnitude data [8]. Since intensity inhomogeneities (e.g., due to multi-channel signal reception or Tx-field variation) cause considerable difficulties in image segmentation both the arterial and venous datasets were post-processed: ToF data was homogenized by applying a bias field that was estimated using FSL (FMRIB, Oxford, UK). Signal variations in SWI data were suppressed by subtracting 3D median filtered SWI data from the original SWI volume. This also minimized contrast from large scale anatomical structures and improved venous delineation [9].

Segmentation: The employed level-set method relies on a time dependent evolution function ϕ in image space that evolves in three dimensional space, combining both boundary and region information of the input data I . The evolution is described by [4]

$$\frac{\partial \phi}{\partial t} = |\nabla \phi| \cdot \left[\alpha \cdot (I - \mu) + \beta \cdot \left(\nabla g \cdot \frac{\nabla \phi}{|\nabla \phi|} \right) + \beta \cdot g \cdot \text{div} \left(\frac{\nabla \phi}{|\nabla \phi|} \right) \right], \quad (1)$$

where α and β are weights to balance between regional and boundary information, respectively. μ is the lowest grey level to be considered for evolution and g is a boundary feature map. The first, second and third term in Eq. 1 describe propagation, advection and curvature flow of the curve, respectively. The boundary feature map was obtained by applying a 3D multi-scale quadrature filter [10] to the input data (ToF or median filtered SWI). As starting condition for the level-set algorithm the initial evolution function was defined by grey level thresholding in combination with morphological operations (erosion, dilation) based on ToF data and on the vessel enhanced median filtered SWI volume [11].

RESULTS

The segmentation results for the arterial and venous vasculature are presented as shaded surface representations in figure 1a and 1b, respectively. Based on ToF information the sagittal sinus was misclassified as artery, whereas the interhemispheric fissure was falsely detected as venous vessel. Because of the simultaneous data acquisition of ToF and SWI both data sets are intrinsically registered. Thus, the segmented arterial and venous vessel trees can be merged into one 3D model of the cerebral vasculature (Fig 2). The geometrical relationship between arteries and veins is clearly visible in the arterio-venous model (see Fig 2b).

DISCUSSION

We have presented initial results for arterial and venous vessel segmentation based on ToF and SWI data. Exact voxel-based classification of arterial and venous vasculature based on ToF-SWI data is challenging. For instance, venous saturation pulses in ToF acquisition are not able to completely remove all venous contributions (e.g., sagittal sinus, sinus rectus). The interhemispheric fissure is another critical structure which is characterized by grey levels similar to veins in both susceptibility weighted magnitude and phase information. Computing the medial axes of the segmented data and analyzing the cross-section perpendicular to the medial axes may help to identify voxels belonging to the interhemispheric fissure. Future research will focus on improvement of vessel segmentation and quantitative description of the segmented blood vessel network based on vessels' centreline (curvature, torsion, tortuosity), radii, and surfaces.

REFERENCES

1. Kirbas C and Quek FKH. ACM Comput. Surv. 2004; 36(2):81-121.
2. Lesage D et al. Med Image Anal. 2009; 13(6):819-45.
3. Manniesing R et al. Med Image Anal. 2006;10(2):200-14.
4. Zhang Y et al. Proc. of the 5th International Conference Biomedical Visualization: information Visualization in Medical and Biomedical informatics. MEDIVIS 2008; 00:71-76.
5. Deistung, A et al. J Magn Reson Imaging. 2009; 29(6):1478-84.
6. Noll DC et al. 1991;10(2):154-63.
7. Jin Z et al. J Magn Reson Imaging. 2008; 28(2):327-33.
8. Reichenbach JR and Haacke EM. NMR Biomed. 2001; 14(7-8):453-67.
9. Kholmovski E and Parker D. Proc. of ISMRM. 2006; 14:810.
10. L  then G et al. Proc. of 19th International Conference on Pattern Recognition. Tampa, FL, USA: IAPR, 2008.
11. Frangi A et al. MICCAI'98, LNCS 1496. 1998:130-137.

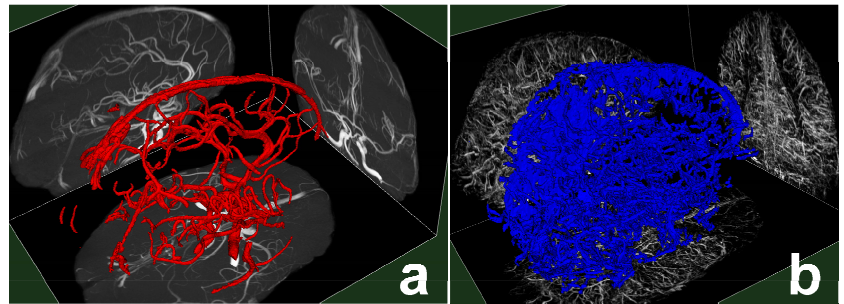


Figure 1: Shaded surface rendering of the segmented arterial (a) and venous (b) vessel trees.

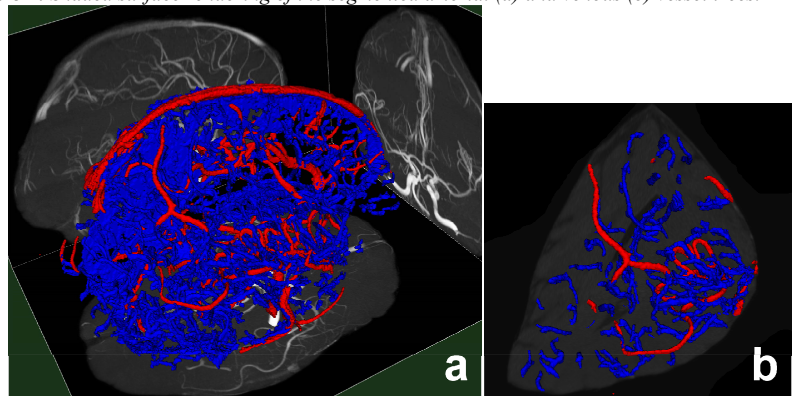


Figure 2: The arterial and venous vessel trees were merged into a 3D model of the whole cerebral vasculature (a) and a small section (b).